

EXPLORATION FOR URANIUM AND THORIUM MINERALIZATIONS AT WADI UM LASEIFA AREA, CENTRAL EASTERN DESERT, EGYPT: USING REMOTE SENSING TECHNIQUE

T. M. Ramadan^a, S. A. El Mongy^b and S. Salah El Dein^a,

^aNational Authority for Remote Sensing and Space Sciences, Egypt,, ramadan_narss2002@yahoo.com

^bNational Center for Nuclear Safety and Radiation Control²

KEY WORDS: Remote sensing, Uranium mineralizations, Airborne radiometric data, Eastern Desert, Granitic rocks, Radiometric materials, Gamma ray spectrometry

ABSTRACT:

This research aims at integrating airborne radiometric and remote sensing satellite data to prospect for radioactivity of the rocks at Wadi Um Laseifa, located in the Central Eastern Desert of Egypt. The study recorded some uranium anomalies along NNE-SSW trending fault zones within the granitic rocks. These occurrences are associated with alkali granites, pegmatitic and manganese veins, trachytic dykes (Gabal Hamrat Ghanam, Gabal El Delihmi, Gabal Nusla and Gabal Abu El Tiyur). Gamma ray spectrometer measurements for representative samples indicate the presence of U up to 17.2 ppm in the trachytic dykes, 12 ppm in the pegmatites and 9 ppm in the manganese veins. Results demonstrate the accuracy of airborne radiometric data and the suitability of remote sensing techniques as a powerful tool in exploration for radioactive materials.

1. INTRODUCTION

The study region lies in the central part of the Eastern Desert of Egypt between Lat. 25° 30' and 25° 55' N and Long. 34° 00' and 34° 40' E. This study aims at integrating airborne radiometric and Landsat Thematic Mapper (TM) data for detecting radioactive anomalies in this area.

Several authors used airborne geophysical data for geological mapping and regional exploration (Misener, et al., 1985, Reeves, 1985 and Ramadan and Sultan, 2003). The radioactive mineralizations of the Egyptian Eastern Desert have been studied by many authors, the most recent studies are carried out by El Ghawaby, 1973, El Shazly, et al., 1973 & 1974), Ammar et al. (1991), El Rakaiby, (1995), Ammar, (1997) and Ramadan et al. (1999).

The study area has been regionally mapped before by Sabet, (1961), Dardir, (1968), Sabet et al. (1976), Kamal et al. (1991), EGSM, (1992), El Alfy, (1992) and Ramadan, et al., (1999).

In the present work, the airborne radiometric maps for the investigated area were processed to show the distribution and intensities of uranium (U), thorium (Th) and potassium (K^{40}) within the studied area. These maps were correlated with geologic and structural maps prepared by using Landsat TM images, to show the lithological and structural features.

2. METHODOLOGY

Spatial integration of various data sets such as geological map (1: 100,000 scale), Landsat TM images (1: 100,000 scale) and airborne radiometric data is applied to show the distribution and intensities of uranium (U), thorium (Th) and potassium (K^{40}) within the studied area. Geographic Information System (GIS) model has been designed and implemented based on the intersection of the buffering zones of each input layer.

2.1 Remote sensing analysis

2.1.1 Landsat TM Data: Landsat Thematic Mapper (TM) data for the study area was processed for geological and structural mapping using the ERDAS imagine 8.5 at the NARSS's Image Processing Lab. A single Landsat TM scene (Path 174, Row 42, date 1986) covering the investigated area has been geometrically corrected and radiometrically balanced and digitally processed.

Digital processing of Landsat TM image for the study area generated several products ranging from single band images, false color composite images (7, 4, 2 in RGB), principal component images (4, 2, 1 in RGB) to ratio images (bands 5/7, 5/1 and band 4/3), (4/3, 3/1, 5/7) in R, G, B (scale 1:100,000). Landsat TM images (bands 7, 4, 2) and Principal component analysis of bands 4, 3 and 2 were used for detecting the regional tectonic structures in the study area. Ratio images (5/7, 5/1, 4/3) and (4/3, 3/1, 5/7) in R, G, B were used for lithological discrimination of different rock types. In such images the investigated ultramafic rocks are indicated by green color, the granodiorites are indicated by red to pinky color, the younger granitic rocks are indicated by purple color (Fig. 2).

2.1.2 Airborne Gamma-ray Survey: Wadi Um Laseifa area was included in the airborne gamma-ray spectrometric survey conducted by Aero-Service over a large segment of the central and southern Eastern Desert, Egypt, designated as area-II (Aero-Service 1985). Airborne radiometric data represent measurements of the gamma-ray flux above the earth's surface, caused by the radioactive decay of U, Th and K^{40} with resolution of 200 m. The survey was flown along a set of parallel traverse flight lines oriented in a northeast-southwest direction, at 1 km spacing, while tie lines were flown northwest-southeast at 10 km intervals. The

high-sensitivity multi-channel radiometric measurements were made at 92 meters interval at a nominal sensor altitude of 120 meters terrain clearance, using twin-engine Cessna-404, Titan type aircraft. A high sensitivity 256-Channel airborne gamma-ray spectrometer-having approximately 50 liters NaI (TI) detector was used as the primary sensor elements in the Aero-Service CODAS/AGRS 3000 F computer based digital data acquisition system (Aero Service 1985). The obtained data were displayed in stacked profiles or contour maps, and interpreted visually.

In the present work, airborne radiometric digital data were converted such to images format and different image processing techniques were applied. These images were designed to show intensities distribution of U, Th and K⁴⁰. The preprocessing steps are as follows:

- a- Converting the data of each element (U, Th, K⁴⁰) to an image file with a set of floating (real) density numbers (DN).
- b- Mapping each element image file to the range 0-255 (integer one byte) because the one-byte image file is much easier in processing and manipulation.
- c- Merging the three elements image files to one multi-bands image that could be manipulated and processed as an ordinary image file. The composite color image representing U, Th and K⁴⁰ distribution and intensity, i.e. blue represents high U and poor Th + K⁴⁰, green represents high Th and poor U+K⁴⁰ and red represents high K⁴⁰ and poor U + Th.
- d- Resampling has been made to project the produced image from the Egyptian Transverse Mercator (ETM) system to Universal Transverse Mercator (UTM) system. This process was necessary to achieve compatibility between the two data types, and to ensure the coincidence between the different layers that could be extracted from both types of data. The various layers in this sense could be easily used in GIS technique.
- e- The areas that have uranium to thorium ratio greater than 30 and uranium content greater than 50 ppm have been allocated. This was done by developing a spatial model to discriminate the desired percentage, producing output raster layers that delineate the areas having values greater than 30 and 50 ppm. The output raster layers in this form were used in GIS modeling with combination of the other layers.

2.1.3 Geographic Information System (GIS):

a- System input

The input layers used in this study are mixture of vector and raster layers including:

- Geological and structural vector maps, which have been extracted from the enhanced Landsat TM image.
- Ground truth information as vector layer.
- U/Th raster layer.

b- GIS model

GIS model has been designed and implemented by ARC/INFO (version 7.02) software package and it is based on the intersection of the buffering zones of each input layer.

The controlled parameters governing the buffering zones have been selected to define the most promising radioactive areas as follows:

Geological unit	All units
Structure	100 m far from faults
U	more than 50 ppm
U/Th	more than 30

c- Output decision

The decision of defining the most promising areas of uranium has resulted as an output image. Figure (1) shows the concentrated areas of uranium (U>50 ppm and U/Th >10) superimposed on Landsat TM image using the above selected controlled parameters. These sites lie between Wadi Sharm El Bahari in the north and Wadi Um Greifat in the south.

2.2. Field and laboratory work

Two field trips for scintilometer measurements and sampling of the recorded sites of high radioactivity. Six sites showing anomalous radioactivity > 50 ppm U on the processed airborne radiometric images were prospected in the field by scintillometer and sampled. The scintillometer used is a "SAPHYMO – STEL", type S.P.P.2. NF.

Thin sections and polished surfaces for 30 samples were studied microscopically to reveal the mineralogical composition of the rock units and the hosted radioactive anomalies.

Eighteen rock samples were collected from the 6 sites representing the highly anomalous radioactivity sites. Then, laboratory gamma ray measurements for these samples were carried out using the Hyper Pure Germanium Gamma-Spectrometer (HpGe). The collected rock samples were crushed, sieved and packed in 100 ml volume containers. The containers were then sealed for four weeks to get secular equilibrium between ²³²Th and its daughters. The gamma ray analyses of the samples have been carried out by HpGe detector with 8K multichannel analyzer (MCA). The detector (Canberra type) has 40% efficiency with 1.95 keV resolution at 1332 keV of ⁶⁰Co. The system was energy calibrated by using multi gamma ray sources; ¹³⁷Cs, ⁶⁰Co and ⁵⁷Co. The efficiency of calibration and factors to be used for quantitative calculations of thorium and uranium were carried out. All the measurements have been carried out at the Central Laboratory for Environmental Measurements, National Center for Nuclear Safety and Radiation Control.

Uranium was identified based on its daughter transition, 63 keV of ²³⁴Th. Thorium was determined based on its daughters gamma transitions; 583keV of ²⁰⁸Tl and 911keV of ²²⁸Ac. The activity (A) of ²³⁸U and ²³²Th was calculated by the following equation;

$$A = R \cdot Fn / \rho \quad \text{Bq/Kg} \dots\dots\dots 1$$

where R = the count rate in the specific photo peaks
 Fn = the factor of normalization
 J = the sample density (g/cm³)

The activities (Bq/g) of uranium and thorium were then converted to concentration in ppm (ug/g) by using the following equation:

$$A = (w/A.wt) \cdot Nf \cdot (0.693/T_{1/2}) \dots\dots\dots 2$$

where w = the weight of ²³⁸U and ²³²Th (ug/g)
 A.wt = the atomic weight of U and Th,
 Nf = the Avogadro's number (6.02 x 10²³)
 T1/2 = the half life time of U and Th.

The IAEA's Reference materials were used for quality control of the calculations and results.

3. RESULTS AND DISCUSSION

3.1 Lithologic interpretation

Lithological formations of Wadi Um Laseifa area were identified from the analysis and interpretation of Landsat TM data, as well as the field study. This area is covered by Pan African Precambrian basement rocks and overlain by Phanerozoic sedimentary rocks (Fig. 2).

The Pan African rocks are arranged from oldest to youngest as follows: ophiolitic ultramafic rocks, ophiolitic melange, metavolcano-sedimentary rocks, metavolcanic rocks, gabbro-diorite rocks, granodiorites, Hammamat sediments, calc-alkaline and alkali granites. These rocks are injected by pegmatite and quartz veins as well as felsitic and trachytic dykes.

Phanerozoic rocks are outcropping in the eastern flank of the area and represented by Miocene sediments (Gabal El Rosas, Abu Dabbab, Essel and Sharm El Bahari formations), Pliocene sediments (Gafir, Shagara and Wizr formations), Pliocene (Um Gheig Formation) and Quaternary deposits (Fig. 2).

3.2 Radioactive occurrences

The identified radioactive anomaly sites are classified into three groups according to their main trend and their host rocks.

- The first group trending NNE-SSW and associated with the alkali-granite, trachytic dykes, felsitic plugs and pegmatitic veins at Gabal Hamrat Ghannam, Gabal Dileihimi, Gabal Abu El Tiyur respectively.
- The second group trending NNE-SSW and associated with the manganese veins which injected the granitic rocks at Gabal Abu El Tiyur.

Table (1) gives the concentration of the different radionuclides in ppm for U and Th in ppm of both groups.

- The third group trending NNW-SSE associated with the Miocene sediments at the area between Wadi Sharm El Bahari and Wadi Um Greifat (Ramadan, et al., 1999).

The following is brief description for these sites according to host rocks.

3.2.1 Radioactive associations with the granitic rocks: This type of radioactive anomalies is associated with the alkali-granite, trachytic dykes, felsitic plugs and pegmatitic veins.

a. Gabal Hamrat Ghannam area

This area is covered by granodiorites and intruded by biotite and alkali granites. Several trachytic dykes trending 20° N and cut these rocks. The delineated radioactive anomalies having U > 50 ppm occur within the alkali granite and trachytic dykes in the southern part of Gabal Hamrat Ghannam (Lat. 25° 52' 20" N and Long. 34° 16' 30" E). These trachytic dykes reach up to 50 m in thickness and up to 2 km in length and trending NNE-SSW (Fig. 3). Gamma ray readings of the scintillometer in the granodiorites are ranging from 40 to 50 c/s, from 130 to 150 c/s in the alkali granites and from 160 to 190 c/s in the trachytic dykes at sensitivity 500. The HPG measurements of U and Th in the

trachytic dykes show that the contents of U range from 3.2 to 10 ppm, and Th from 10 to 18 ppm (Table - 1).

b. Gabal Dileihimi area

This area is covered by granodiorites and intruded by biotite and alkali granites. Several felsitic and trachytic dykes cut these rocks and trending 20° N. The delineated radioactive anomalies having U > 50 ppm occur in the alkali granite and trachytic dykes in the northern part of Gabal Dileihimi. Gamma ray readings of the scintillometer in the granodiorites are ranging from 40 to 50 c/s and from 150 to 170 c/s in the alkali granites.

c. Gabal Abu El Tiyur area

This area is covered by biotite and alkali granite. Numerous felsitic dykes trending N-S cut these rocks. The delineated radioactive anomalies having U > 50 ppm occur within alkali granite and felsitic dykes in the northern part of Gabal Abu El Tiyur (Lat. 25° 45' 05" N and Long. 34° 15' 15" E). The readings of the scintillometer in the felsitic dykes are ranging from 175 to 200 c/s.

d. Gabal Nusla area

This area is covered by granodiorites and intruded by biotite and alkali granites. Several felsitic dykes and pegmatitic veins trending 20° N are injected in these rocks. The delineated radioactive anomalies having U > 50 ppm occur within felsitic dykes and pegmatitic veins at the northern part of Gabal Nusla (Fig. 3) The readings of the scintillometer in the granodiorites are ranging from 140 to 150 c/s. The HPG measurements of U and Th in the pegmatitic veins show that: the contents of U range from 9.7 to 17.2 ppm, and Th from 23 to 36 ppm (Table - 1).

e. Wadi Maktal Mohamad:

A radioactive anomaly, where U exceeds 50 ppm, is recorded at the upper reaches of Wadi Abid, representing the northern tributary of Wadi Maktal Mohamad. At this site, a felsite plug cuts the gabbroic rocks and is partially covered with Miocene clastic-carbonate formations. In this felsitic plug, the readings of the scintillometer range from 150 to 160 c/s.

3.2.2 Radioactive anomalies within the manganese veins:

Several manganese veinlets injected the granitic rocks of Gabal Abu El Tiyur at its eastern side trending N-S. These veins reach up to 2 m length and 3 cm width. The readings of the scintillometer are ranging from 175 to 200 c/s. The measurements of U and Th in the manganese veins show that: the contents of U range from 0.9 to 9 ppm and Th is less than the detection limit of the gamma spectrometer (Table - 1).

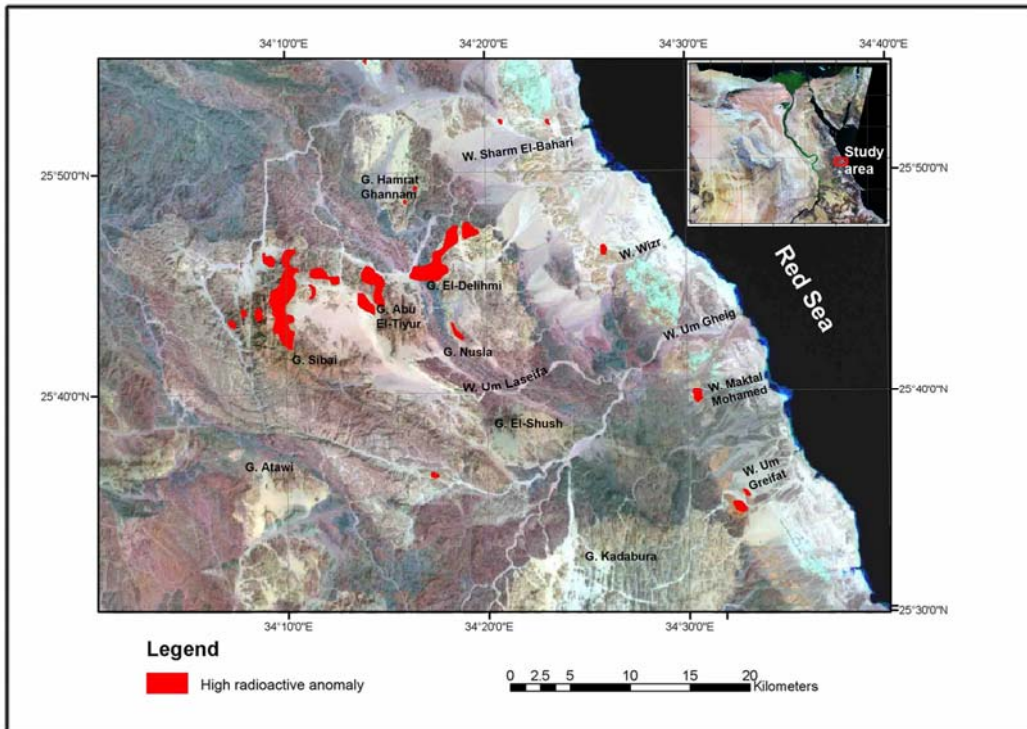


Figure 1: $U > 30$ and $U/Th > 10$ (red) distribution and intensity map superimposed on Landsat TM image of the study area

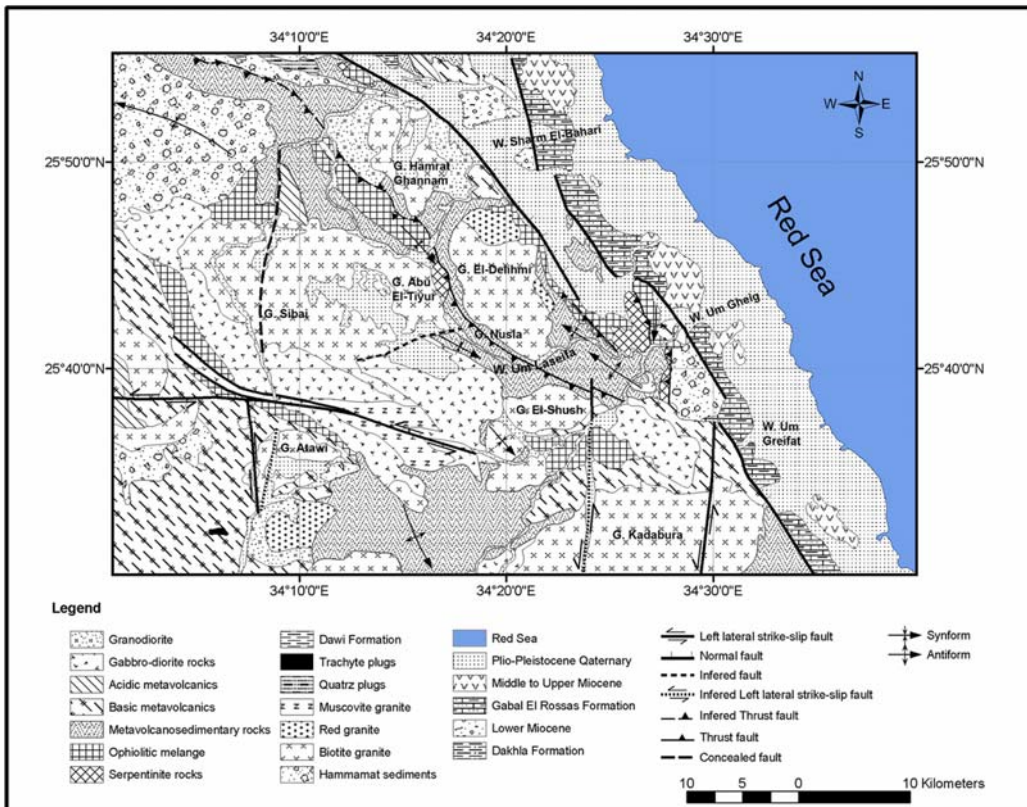


Figure 2. Geological map of the study area, modified after EGSM 1992.



Figure 3. Photograph showing pegmatitic vein (P) injected in the younger granites at Gabal Homret Ghannam



Figure 4. Photograph showing felsite dyke (F) cut the metavolcano-sedimentary rocks, northwest of Gabal Nusla

Ser. No.	Site Code	Rock type	Scint. Readings c/s	^{238}U Bq/Kg	^{238}U ppm	^{232}Th Bq/Kg	^{232}Th ppm
1	S5	Red granite	160	70.9 +34	5.8 ppm	71.8+11	17.8 ppm
2	S9	Red granites	250	123.8 +45	10 ppm	55.1+8	13.6 ppm
3	S13	Felsite dyke	175	38.9 +15	3.2 ppm	41.8 +8	10.3 ppm
4	UL1	Trachyte dyke	250	211 +29	17.2 ppm	120.8+7.2	30 ppm
5	UL2	Trachyte dyke	200	118+47	9.6 ppm	116.2+12	29 ppm
6	UL4	Pegmatite vein	200	120.+37	9.8 ppm	93 +15	23 ppm
7	UL5	Pegmatite vein	230	144.7 +89	12 ppm	145.2 +16	36 ppm
8	Mn1	Manganese vein	200	110.1 +57	9 ppm	<DL	<DL
9	Mn2	Manganese vein	120	11.2 +3	0.9 ppm	<DL	<DL

*DL: Detection limit of the gamma spectrometer

S = Trachytic dykes of Hamrat Ghanam area

UL = Fesitic dykes of Umm Laseifa area

Mn = Manganese veins of Gabal Abu El Tiyur area

Table 1. Concentration of ^{238}U and ^{232}Th in ppm of the study area

4. CONCLUSION

The present work revealed the presence of several new radioactive sites in the Central part of the Eastern Desert. These occurrences are located along N-S and NNE-SSW trending fault zones, within the granitic rocks and contrary to those recorded by Ramadan et al., (1999) which occur along NW-SE trending fault zones, within the Miocene clastic-carbonate sediments. The radioactive anomalies are associated with the alkali granites, pegmatitic and manganese veins, trachytic dykes at Gabal Hamrat Ghanam, Gabal El Delihmi, Gabal Nusla and Gabal Abu El Tiyur respectively

Detailed chemical and mineralogical studies for these uraniumiferous sites are recommended. The results of the present study demonstrate the accuracy of airborne radiometric data as well as the suitability of the remote sensing technique for exploration for radioactive material.

ACKNOWLEDGEMENT

The authors would like to thank Prof. M. M. Hassaan, Al Azhar University and Prof. I. El Kassas, NARSS for their sincere help and discussions.

References

- Aero-Service, 1985. Airborne gamma-ray spectrometer and magnetometer survey of the Eastern Desert of Egypt, area-II, Interpretation report, Aero Service Division, Western Geophysical Co. of America, Houston, Texas, USA, 127 p.
- Ammar, A. A., El Sirafe A. M. and El Kattan E. M., 1993. Airborne geochemical and structural investigation of the Precambrian copper-bearing rocks, Hammash District, South Eastern Desert, Egypt. *Annal. of the Geol. Surv. of Egypt*, Vol. XIX, pp. 467-486.
- Dardir, A.A., 1968. A Proposed Classification for the Miocene and Post-Miocene sediments along the Egyptian Red Sea Coastal Plain. *Geol. Surv., Egypt., Cairo, Egypt.*
- Bodonsky, D., 1996. Nuclear Energy; Principles, Practices and Prospects, American Institute of Physics, NY, USA.
- El Alfy, Z., 1992. Geological studies on the area north of Gabal Abu El-Tiyur, central Eastern Desert, Egypt. Ph. D. Thesis, Am Shams Univ., Cairo, Egypt. 177 p.
- El Etr, H. A., Yousif, M. S. and Dardir, A. A., 1979. Utilization of Landsat images and conventional aerial photographs in the delineation of some aspects of the geology of the Central Eastern Desert, Egypt. *Annal. Geol. Surv. Egypt*, Vol. IX, pp 136-162
- El Ghawaby, M. A., 1973. Structures and radioactive mineralization of Wadi Zeidun area, Eastern Desert, Egypt; Ph. D. Thesis, Ain Shams Univ., Cairo, Egypt.
- El Khadragey, A. A., 1980. Studies of sedimentology and geochemistry in some Miocene deposits between Quseir and Mersa Alam, Eastern Desert, Egypt. M. Sc. Thesis, Al Azhar Univ., Cairo, Egypt. 198 p.
- El Rakaiby, M. L., 1988. The tectonic lineaments of the basement belt of the Eastern Desert, Egypt. *Egyptian Journal. Geol.*, Vol. 32, pp. 77-95.
- El Rakaiby, M. L. 1995. The use of enhanced Landsat TM image in the characterization of uraniumiferous granitic rocks in the Central Eastern Desert of Egypt. *Int. J. Remote Sensing*, Vol. 16, (6), pp. 1063-1074.
- El Shazly, E. M. and El Ghawaby, M. A., 1974. Tectonic analysis of Wadi Zeidun area and its application in localizing radioactive mineralization in the Central Eastern Desert, Egypt. 2nd Arb. Conf. Miner. Resour., Jeddah, Saudi Arabia. pp. 20-43.
- El Shazly, E. M., El Kassas, I. A. and Mostafa, E. M., 1977. Economic Geology and Mineralogy, Comparative Fracture analysis and its relation to Radioactivity in the Pink Granite of Umm Had Pluton, Central Eastern Desert. 16th Annu. Meet. Geol. Soc., Egypt, pp. 12-21.
- Greiling, R. O., El Ramly, M. F. and El Akhal, H., 1985. Tectonic evolution of the northwestern Red Sea margin as related to Basement structure, *Tectonophysics*, Vol. 153, pp. 179 - 191.
- Hassaan, M. M., 1990. Studies on lead-zinc sulphide mineralization in the Red Sea coastal zone, Egypt. Proceedings of the eighth Quadrennial IAGOD Symposium: pp. 835-847.
- Kamal El Din, G. M., Khudeir, A. A. and Greiling R. O., 1991. Tectonic evolution of the Pan-African gneiss culmination, Gabal El Sibai area, Central Eastern Desert, Egypt. *Zbl. Geol. Palaont. Teil. 1, H (11)*, pp. 2637-2640, Stuttgart.
- Misener, D. J., Refold, S. W. and Holroyd, M., 1985. Ternary colour plotting of three radio-element spectrometer data. Pro. 54th annual meet. Soc. of Exploration Geophysicists (Hyderabad), Vol. 4, No. 3, pp. 41-44.
- Ramadan, T. M., El-Lithy, B. S., Nada, A. and Hassaan, M. M., 1999. Application of remote sensing and GIS in prospecting for radioactive minerals in the Central Eastern Desert of Egypt. *Egypt. Jour. Remote Sensing and Space Sci.*, Vol.2, pp. 141-151.
- Ramadan, T. M. and Sultan, A. S., 2003. Integration of geological and geophysical data for the identification of massive sulphide zones at Wadi Allaqi area, South Eastern Desert, Egypt. (in press).
- Reeves, C. V., 1985. Airborne geophysics for geological mapping and regional exploration. *ITC Journal*, Vol. 3, pp. 147- 161.
- Sabet, A. H., 1961. Geology and mineral deposits of Gabal El-Sibai area, Red Sea hills, Egypt. Ph. D. Thesis, Leiden State Univ., Netherlands.
- Sabet, A. H., Tsogoev, V. B., Bordonosov, V. P., Beloshitsky, V. A., Kuznetsov, D. N. and El-Hakim, H. A., 1976. On some Geological and Structural Peculiarities of the localization of the polymetal mineralization of the middle Miocene sediments of the Red Sea Coast. *Annals Geol. Surv. Egypt*, V. VI. Pp. 223-236.
- Sultan, M., Arvidson, R. E. Duncan, I. J., Stern, R. J. and El Kaliouby, B., 1988. Extension of the Najd Shear System from Saudi Arabian to the Central Eastern Desert of Egypt based on integrated field and Landsat observation. *Tectonics*, Vol. 7, pp. 1291-1306.